ELSEVIER

Physica C 272 (1996) 13–20

PHYSICA C

Possible interpretation on the existence of an anomalous inversion of some ZFC and FC transport characteristics in YBCO and BSCCO ceramic superconductors

J. López *, P. Muné [1], S. García, E. Altshuler

Superconductivity Laboratory, IMRE, Faculty of Physics, University of Havana, 10400 Havana, Cuba

Received 29 July 1996; revised manuscript received 30 September 1996

Abstract

We performed a comparative and systematic study of voltage versus current and critical current versus applied magnetic field characteristics measured in zero field cooling (ZFC) and field cooling (FC) conditions, in YBCO and BSCCO 2223 ceramic superconductors. We found an anomalous inversion of ZFC and FC curves at low applied magnetic fields and temperatures in several BSCCO samples; i.e., ZFC curves showed stronger superconductivity than the FC ones. This is in clear contrast to YBCO ceramics. Besides, the studied curves for BSCCO ceramics presented a much weaker dependence on cooling conditions than the ones corresponding to YBCO. We also made a semi-quantitative interpretation of the anomalous inversion through the investigation of the internal magnetic field.

Keywords: Transport characteristics; ZFC and FC conditions; YBCO and BSCCO 2223 ceramics; Internal magnetic fields

1. Introduction

The comparative study of curves such as voltage versus current, magnetization versus temperature and susceptibility versus temperature, measured in zero field cooling (ZFC) and field cooling (FC) conditions has proved to be a very successful tool in the investigation of high temperature superconductors. For instance, it provides the main procedure to determinate the irreversibility line [1,2].

FC curves have usually presented "better" superconducting properties than the corresponding ZFC ones. However, a sizable quantity of articles that partially contradict this point have recently appeared in the literature. For example, Iga et al. [3] found for temperatures close to the critical one in BSCCO superconductors that the ZFC magnetization versus magnetic field curve was unexpectedly above the FC one. Also Bekeris et al. [4], studying ac susceptibility versus temperature and magnetic field in a lanthanum-based sample, detected that the ZFC curves were above the corresponding FC ones. However, they did not see the same effect in dc susceptibility studies.

In two previous articles [5,6] we presented an anomalous inversion between ZFC and FC voltage versus current curves in BSCCO ceramics and a systematic and comparative study of these character-

* Corresponding author. E-mail: Altshul@tinored.cu.

[1] On leave from: Department of Physics, University of Oriente, Las Américas, Santiago de Cuba, Cuba.

PII S0921-4534(96)00586-2

istics with the analogous YBCO ones. Here we partially review these topics, trying to understand the origin of the differences between these superconducting families. We also attempt a semi-quantitative interpretation of the anomalous inversion through the investigation of the internal magnetic field.

2. Experimental

We prepared $YBa_2Cu_3O_{7-\delta}$ (YBCO) and $Bi_{1.6}Pb_{0.4}Sr_2Ca_2Cu_3O_y$ (BSCCO) ceramic samples using the standard method. For YBCO, we mixed in stoichiometric proportions high purity powders of Y_2O_3,$BaCO_3$ and CuO. These rough materials were calcinated during 16 h at 900, 920 and 940°C, respectively. At each step we grounded the resultant powders in a mill. Afterwards the powders were pressed in disks and sintered at 950°C for another 16 h. The cooling rate was 1°C/min to room temperature in an oxygen atmosphere. For BSCCO we mixed stoichiometrically high purity powders of Bi_2O_3, PbO_2, $CaCO_3$, $SrCO_3$ and CuO. These were homogenized and calcinated at 820°C for 24 h. Later, they were grounded, uniaxially pressed and sintered at 850°C. The cooling rate in the furnace was 1°C/min again.

Finally, we cut from the disks slab-like samples with typical dimensions of $1.00 \times 1.25 \times 10$ mm^3 (YBCO) and $1.10 \times 2.00 \times 10$ mm^3 (BSCCO). Transport measurements were performed by the four-probe method. Silver contacts were diffused into the ceramic bars and the final resistance was less than 1 Ω in each case. The critical temperature for the studied samples, defined as the inflection point at the transition in the resistivity versus temperature curves, was found to be 91 and 108 K for YBCO and BSCCO, respectively.

Critical current density versus applied magnetic field (J_c–H) and voltage versus current (V–I) curves were measured in ZFC and FC conditions [5]. Between a ZFC point or curve measurement and a FC one (and vice versa) the samples were heated well above their critical temperatures. Voltage and current were measured with 1 uV and 1 mA accuracy, respectively. A 10^{-5} V/cm electric field criterion for the critical current determination was used. The external magnetic field was generated by a long solenoid up to 500 Oe. The temperature was chosen by a Lake Shore 330 control with a maximum 0.01 K resolution and varied from 77 K up to 125 K.

3. Theory

Eq. (1) shows the critical current density dependence on the applied magnetic field for a ceramic sample. This was modeled as the envelope of the superposition of several Fraunhofer-like patterns, each one typical of a single short Josephson junction [7]. We are going to use these expressions in the fitting curves of Fig. 2.

$$J_c = J_0 \left| \frac{\mathrm{sen}(\pi\Phi/\Phi_0)}{(\pi\Phi/\Phi_0)} \right|, \quad |\Phi| \le \tfrac{1}{2}\Phi d0,$$

$$J_c = J_0 |\Phi_0/\pi\Phi|, \quad |\Phi| > \tfrac{1}{2}\Phi_0, \qquad (1)$$

where Φ_0 is the magnetic flux quantum, J_0 is the Josephson current density for $\Phi = 0$ and $\Phi = 2\lambda L \mu_0 H_i$. Here, λ is the London penetration depth of the grains, L is the Josephson junction average length, μ_0 is the free space magnetic permeability and H_i is the intergranular magnetic field. The H_i values strongly influence the transport properties in ceramic superconductors. Eq. (2) shows its dependence on the external magnetic field, H, the magnetization of the neighbor grains, M, and a geometric factor, G:

$$H_i = H - GM(H_i). \qquad (2)$$

Actually, in a polycrystal there is a distribution of geometric factors G, instead of a single value. Fig. 1a sketches a hypothetical ZFC magnetic flux line distribution between a superconducting grain brick wall array for magnetic fields lower than the first critical field of the grains ($H < H_{c1g}$). Points C and D represent regions of compression and decompression of magnetic flux lines (higher and lower intensities), respectively. Muné et al. [8,9] have shown that they could be mathematically modelled using positive and negative G values. Fig. 1b shows two possible current paths. The first one goes along the $G > 0$ regions and the second along the $G < 0$ ones. We will see that, in the YBCO samples, the current flows more likely through paths including regions of positive G values. However, in BSCCO ceramics the

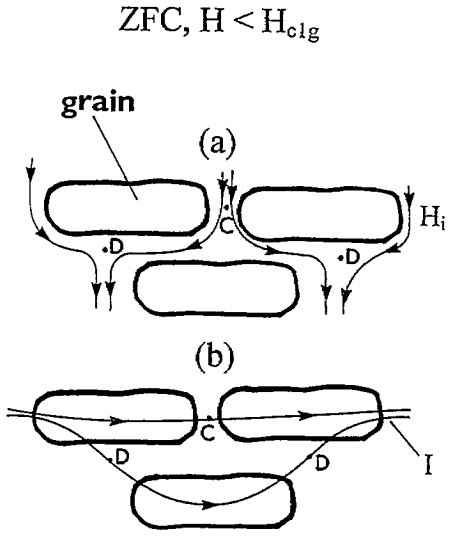

Fig. 1. (a) Hypothetical ZFC magnetic flux lines distribution and (b) two possible current paths through a brick wall array of superconducting grains. Points C and D correspond to regions of positive and negative geometric factors, respectively.

current is more or less equally divided between both kind of paths.

Finally, the magnetization of each grain depends on the internal magnetic field and on the cooling conditions. We use in our simulations the expressions of M from the Bean model, following Müller et al. [7] and Muné [10].

4. Results and discussion

4.1. J_c versus H curves

Fig. 2a and b show the applied magnetic field dependence of the normalized critical current density for the YBCO and BSCCO samples at 78.0 and 95.0 K, respectively. Note that we selected these temperatures in such a way that $T/T_c = 0.8$ in both families. The measurement was done in ZFC (solid circles) and FC (open circles) conditions. In both cases the critical current density decreases as the magnetic field increases. Nevertheless, in contrast to the YBCO ceramic case, where in the middle field the ZFC curve is well below the corresponding FC curve, in BSCCO the two curves always remain very close.

As we showed in a previous article [5], in the BSCCO sample at low magnetic fields the ZFC points are unexpectedly above their corresponding FC ones. At a characteristic magnetic field (16 Oe in Fig. 2b), that we will call anomalous (H_a), the curves intercept. With higher magnetic fields the curves split, but now the ZFC points are below the corresponding FC ones (as in YBCO). Finally, at a given magnetic field that we will call equivalent ($H_a = 100$ Oe in Fig. 2b), or greater, both curves merge into a single one.

The fact that FC curves present better superconducting properties than the corresponding ZFC ones has been interpreted as follows. Flux pinning forces

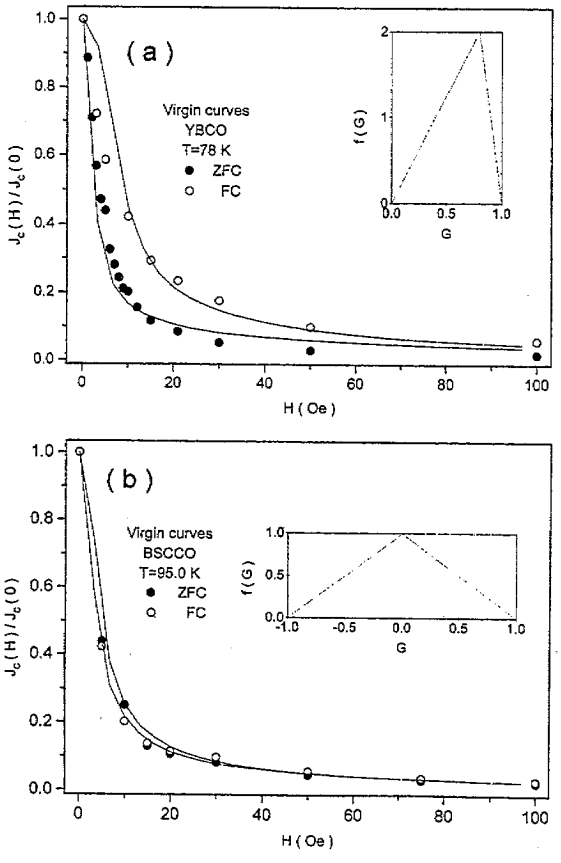

Fig. 2. Normalized critical current density dependence on applied magnetic field for (a) the YBCO ceramic at 78.0 K and (b) the BSCCO ceramic at 95.0 K. Solid and open circles represent the measurement done in zero field cooling (ZFC) and field cooling (FC) conditions, respectively. The insets show the geometric factor distribution functions used in the theoretical fitting (continuous lines).

oppose the expulsion of flux lines from inside the grains in FC conditions. They also oppose the magnetic field penetration into the grains in ZFC. As a result, flux lines are more compressed at the weak links in the ZFC case than in the FC one. Since the junctions determine the transport properties, the critical current is lower in ZFC conditions.

Continuous lines in Fig. 2a and b represent the fitting of the experimental points to an extended intragranular flux trapping model (Section 3). This was developed by Muné et al. [10,11] taking into account, for the first time, the possible existence of negative geometric factors and a two-dimensional series–parallel array of Josephson junctions.

The fitting procedure is the following. First, we find from the flux trapping curve (see below) the first critical magnetic field of the grains (H_{c1g}) and the saturation magnetic field, H. Then we calculate $H^* = (H_s - H_{c1g})/2$ (the magnetic field for which the flux lines completely penetrate the grain following the Bean model). Both H_{c1g} and H^* will be fixed parameters. Then, we vary, simultaneously for the ZFC and FC curves, $H_0 = \Phi_0/(2\lambda L \mu_0)$, the first critical magnetic mean field of the junctions and the geometric factor distribution function, $f(G)$, until a good fit is achieved.

The insets in the upper right part of Fig. 2a and b show the distribution geometric factor functions, $f(G)$, used in each case. It is very important to note that, in the YBCO sample, the G values are only positive with the peak at 0.8. However, in the BSCCO one, the G values are distributed in the whole interval -1 to 1. Here, the highest probability is at $G = 0$. The parameters H_0, H_{c1g} and H^* at the corresponding temperatures for YBCO were 15, 20 and 55 Oe and for BSCCO were 8, 10 and 42 Oe, respectively. Although H_0, H_{c1g} and H^* do not vary very much between YBCO and BSCCO, their corresponding distribution functions of geometric factors are quite different.

4.2. V versus I curves

Figs. 3a and b show the systematic variations with an applied magnetic field of the voltage versus current curves. They were measured at constant temperatures of 78.0 K in YBCO and 95.0 K in BSCCO, respectively. Each type of symbol represents a given

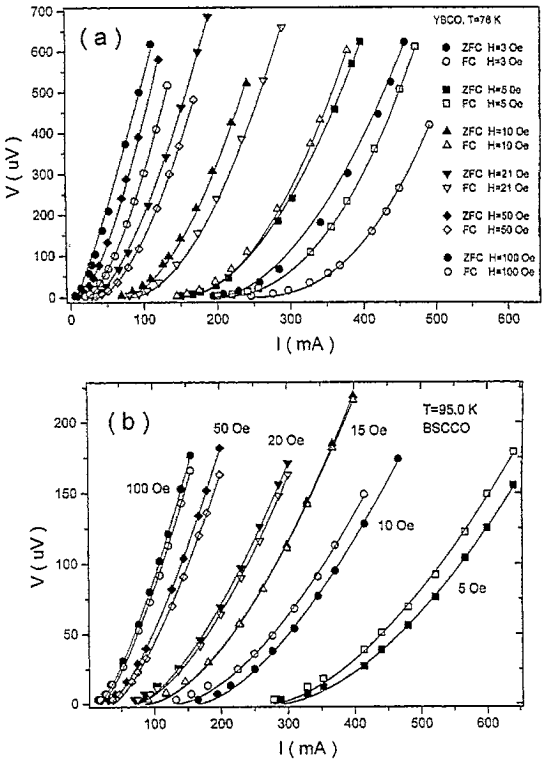

Fig. 3. Voltage versus current curves of (a) YBCO and (b) BSCCO ceramics in different magnetic fields and cooling conditions (ZFC, solid symbols; FC, open symbols). Temperatures were fixed at 78.0 and 95.0 K, respectively. Continuous lines represent the fitting of experimental data to a power law.

fixed applied magnetic field in ZFC (solid) and FC (open) conditions.

Continuous lines represent the fitting of a one-parameter power law [5,12] to the experimental points. The general agreement in the whole field and temperature ranges is remarkable in both samples. The same qualitative variation with magnetic field and temperature holds again, but now for a whole curve instead of a single point of the J_c versus H characteristics. Note that all the points of each curve in a pair are systematically either above or below the corresponding curves but do not cross each other.

In the YBCO ceramic, the ZFC V versus I curves present always worse superconducting properties than the corresponding FC curves. In other words, $J_{c\,ZFC} < J_{c\,FC}$ and, therefore, now the ZFC V versus I curves are above the FC ones for the same magnetic field. We should be careful to not confuse the rela-

tive position between ZFC and FC curves in the J_c versus H and V versus I plots.

Besides, the separation in the YBCO sample between ZFC and FC curves first increases and later decreases until they overlap at higher magnetic fields. Another interesting point is that the FC curves at 5, 21, 50 and 100 Oe present better superconducting properties than the ZFC ones at 3, 10, 21 and 50 Oe, respectively. These results agree quite well with a similar study of Barroso et al. [13] in the YBCO family where the yttrium was replaced by gadolinium.

On the other hand, in the BSCCO sample both ZFC and FC curves for the same magnetic field are always very close. Note that, unlike YBCO, there are no other curves measured at a different magnetic fields appearing between a pair of ZFC and FC curves. This suggests that the magnetic field itself is more important than the cooling conditions in these characteristics.

Reinforcing the previous results in Fig. 2b, at low magnetic fields, the whole ZFC curves present better superconducting properties than the FC ones (anomalous inversion) in the studied temperature range. In other words, the ZFC curves are below the FC ones in the V versus I plot (ZFC above FC in J_c versus H).

In Fig. 4 (analogous to Fig. 2b) at a typical magnetic field, H_a, both ZFC and FC curves overlap. When greater magnetic fields are applied they split, but now the ZFC curves are above the corresponding FC ones (as in YBCO). Finally, the curves merge once more at a magnetic field equal to H_a and

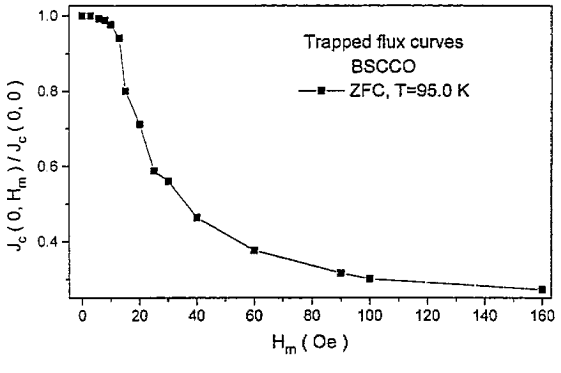

Fig. 4. Typical ZFC magnetic flux trapping curve for the BSCCO sample at 95.0 K (see text).

remain together for higher fields. Although here we only report measurement in one BSCCO sample, we found similar results, including the anomalous inversion, in several others.

4.3. Phase diagram

We measured the flux trapping curves [14] in ZFC conditions at different temperatures [10]. Fig. 4 shows a representative example for the BSCCO ceramic at 95.0 K. The results could allow us to correlate the variations of the anomalous and equivalent magnetic fields with intragranular parameter of the sample, such as H_{c1g} and H_s. We have already used these values in the fitting of the J_c versus H curves.

The measuring procedure is the following. The sample is cooled down until the desired temperature in ZFC conditions. Then, the magnetic field is increased to a value H_m, which is applied for several seconds and subsequently suppressed afterwards. At that moment, we measure the critical current density and plot its value versus H_m. Finally, we normalize the whole curve to J_c at $H_m = 0$.

As Altshuler et al. showed [14], the critical current density does not decrease for small H_m values. That is because the magnetic field lines in ZFC conditions do not remain trapped in the sample when we remove the magnetic field. However, starting from $H_m = H_{c1g}$, the magnetic flux lines penetrate the grains and, after the external magnetic field source is turned off, some flux remains trapped in the grains. Consequently, the critical current density decreases when $H_m > H_{c1g}$ and helps us to identify the *first critical field of the grains*. On the other hand, at higher fields ($H_m > H_s$) the critical current density no longer drops. In other words, the grains capability to trap magnetic field lines saturates. We call H_s the *saturation magnetic field*.

Fig. 5 illustrates the H_a and H_s dependence with temperature (which we will call anomalous and equivalent lines, respectively) for our sample. Both curves increase with decreasing temperature, the first at low field values, and the second at higher ones. Actually, the accuracy of these points strongly depends on the overlap criterion taken. Nevertheless, we just want to show here that these two curves define three different sectors in the H versus T phase diagram: one above the H_a line, where the

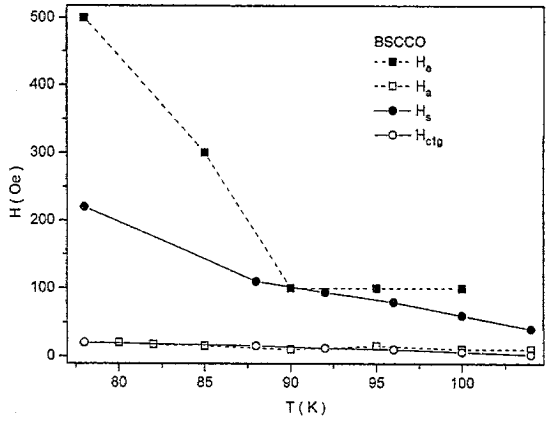

Fig. 5. Representation of the equivalent magnetic field (solid squares), anomalous magnetic field (open squares), saturation field (solid circles) and the first critical field of the grains (open circles) curves in a magnetic field versus temperature phase diagram for the BSCCO ceramic. Lines represent only guides to the eyes.

ZFC and FC curves are completely equivalent, another in between the H_a and H_s lines (normal region) and below the H_a line (anomalous region). On the other hand, we could find only the first two regions for the YBCO ceramics.

Fig. 5 also shows, as a reference, the change of the intragranular parameters H_{clg} and H_s with temperature taken from the flux trapping curves. It is quite important to note the overlapping of the H_{clg} and H_a lines. This reflects the fact that the magnetic field has not penetrated the grains in ZFC conditions when the anomalous inversion is taking place. Besides, the H_s line is below the H_a one, revealing that the grain capability to trap magnetic flux lines is saturated when the ZFC and FC curves overlap.

Similar results, except for the anomalous inversion, were reported by Miu in BSCCO 2223 ceramics [15]. He interpreted them in terms of pinning energy differences between these two cooling conditions. The magnetic field value above which the curves overlapped was assumed to be the intragranular irreversibility value at that temperature.

However, in our sample the pinning energies do not drop to zero at H_s. For example, at 95.0 K they decrease only to about two thirds of the corresponding value at zero magnetic field [5]. This indicates that the equivalent line is actually below the depinning one. We believe that the ZFC and FC curves merge at H_s because their mean values of the internal magnetic field in the array of weak links are similar. At this field value, the main contribution comes from the external applied field rather than from the magnetization of the grains (which is cooling-condition dependent), see Eq. (2).

4.4. Internal magnetic field

In our opinion, the main difference between YBCO and BSCCO curves are due to the morphology of the grains in both systems. As the fitting of the curves in Fig. 2 shows, in the YBCO sample, the distribution of geometric factors G is only positive (flux line compression). Meanwhile, the BSCCO ceramic also includes a region of negative G values (flux line decompression).

Eq. (3) shows the internal magnetic field in a Josephson junction for $H_i < H_{clg}$ and increasing fields calculated following Refs. [7,10].

$$H_i = H/(1-G), \quad \text{ZFC},$$

$$H_i = \frac{H^*}{G} + \sqrt{\left[\left(\frac{H^*}{G}\right)^2 - 2\frac{H^*}{G}H\right]},$$

$$\text{FC and } G > 0, \tag{3}$$

$$H_i = H, \quad \text{FC and } G = 0,$$

$$H_i = \frac{H^*}{G} - \sqrt{\left[\left(\frac{H^*}{G}\right)^2 - 2\frac{H^*}{G}H\right]},$$

FC and $G < 0$.

Fig. 6 shows an example of how the internal magnetic field changes with the applied one. We present ZFC and FC curves using positive ($G = 0.5$) and negative ($G = -0.5$) geometric factors for the BSCCO ceramic with $H^* = 42$ Oe and $H_{clg} = 10$ Oe.

In both cases (ZFC and FC) the existence of $G < 0$ reduces the internal magnetic field. As a result the critical current densities decrease more slowly as compared to the positives G case. Besides, if $G > 0$, H_i in ZFC is greater than in FC. This causes the curves measured in ZFC to lie below the FC ones in a J_c versus H plot. However, if $G < 0$, H_i in ZFC is smaller than in FC and therefore gives rise to the anomalous inversion.

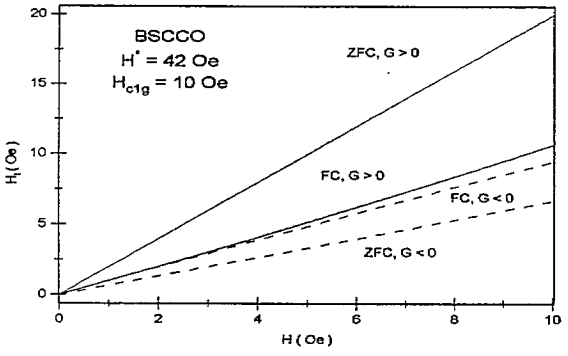

Fig. 6. Internal magnetic field dependence on the applied field in the BSCCO ceramic for $H_i < H_{c1g}$. Continuous and dashed lines represent the calculated field values using positive and negative geometric factors, respectively. ZFC and FC conditions are also indicated.

The distribution of the internal magnetic fields in the intergranular regions strongly influences the critical current that flows through a ceramic superconductor. Our BSCCO sample shows both positive and negative geometric factors. Therefore, the actual H_i curves for the whole sample will be a sort of average between different G values for the same cooling condition. As can be seen in Fig. 3b, this brings the ZFC and FC curves very close. Although not shown here for simplicity, the same conclusion is valid for other magnetic field intervals besides $H_i < H_{c1g}$.

On the other hand, in the YBCO sample the geometric factor distribution is only positive. Therefore, here the difference between ZFC and FC curves will be more evident than in the BSCCO case I. In the same way, as no negative geometric factors are present, we will not find the anomalous inversion.

Another fact to take into account is that the previous expressions allowing us to calculate the internal magnetic fields do not include the existence of Abrikosov vortices trapped perpendicular to the junctions. Gubankov et al. [16] showed, in artificial Josephson junctions, that these vortices distorted the Fraunhofer-like pattern of the J_c versus H curves. However, the trapping of perpendicular Abrikosov vortices is possible in FC even for very small magnetic fields, but in ZFC it can happen just for magnetic fields higher than a characteristic one (of the same order than our H_{c1g}). This will cause an additional decrease of the critical current in the region of $H < H_{c1g}$ in the FC case, but not in the ZFC one. We believe that this asymmetric behavior between ZFC and FC curves could also be responsible of the anomalous inversion. The overlapping in the phase diagram of Fig. 5 of the H_{c1g} and H_a lines also reinforces this point.

5. Conclusions

We measured ZFC and FC critical current density versus applied magnetic field curves in YBCO and BSCCO 2223 ceramics. In contrast to YBCO, where the ZFC curves are well below the FC curves in BSCCO they are always very close. More so, at low magnetic field values, the ZFC curves appear unexpectedly above the FC ones. The fitting of these curves shows that the geometric factor distribution functions are quite different between YBCO and BSCCO ceramics. However, intrinsic parameters such as H_0, H_{c1g} and H^* do not change very much between them.

Confirming previous studies in the YBCO family, the ZFC voltage versus current curves always show worse superconducting properties than their counterparts in FC. Indeed, some FC curves measured at a higher magnetic field than other ZFC curves, show better transport characteristics.

On the other hand, in the BSCCO sample both ZFC and FC voltage versus current curves are always very close. This indicates that the magnetic field is more important here than the cooling conditions. Besides, as in the J_c versus H plot, the relative position between ZFC and FC curves at low magnetic field values appears anomalously inverted. This irregularity disappears for magnetic fields higher than H_a, which we found to be equal to H_{c1g}.

Finally, we estimated the mean internal magnetic fields in the BSCCO ceramic for $H_i < H_{c1g}$. Our results show that when we use both positive and negative geometric factors, the difference between the ZFC and FC curves decreases. Furthermore, when the geometric factors are negative, the internal magnetic field is lower in ZFC than in FC conditions. This can explain the anomalous inversion mentioned above.

References

[1] Y.S. Song, M. Hirabayashi, H. Ihara and M. Tokumoto, Phys. Rev. B 50 (1994) 16644.
[2] L. Miu, G. Aldica, M. Horobiowski and D. Wlosewicz, J. Superconduct. 4 (1991) 423.
[3] F. Iga, A.K. Grover, Y. Yamaguchi, Y. Nishihara, N. Goyal and S.V. Bhat, Phys. Rev. B 51 (1995) 8521.
[4] V. Bekeris, H. Ferrari, C. Acha, P. Levy, G. Polla and G. Leyva, Physica C 234 (1994) 49.
[5] J. López and P. Muné, Physica C 261 (1996) 173.
[6] J. López, P. Muné and S. García, submitted to Phys. Status Solidi (1996).
[7] K.H. Müller and D.N. Matthews, Physica C 206 (1993) 275.
[8] P. Muné, E. Altshuler, J. Musa, S. García and R. Riera, Physica C 226 (1994) 12.
[9] P. Muné, E. Altshuler and J. Musa, Physica C 246 (1995) 55.
[10] P. Muné, Ph.D. Thesis, University of Havana, Cuba (1996).
[11] P. Muné and J. López, Physica C 257 (1996) 360.
[12] J. López, M. Sc. Thesis, University of Havana, Cuba (1996).
[13] J. Barroso, D. López, F. Pardo and N. Ayoub, paper presented at: The Advanced Workshop on HTc Superconductors and Related Materials (CAB, Argentina, 1993).
[14] E. Altshuler, S. García and J. Barroso, Physica C 177 (1991) 61.
[15] L. Miu, Cryogenics 32 (1992) 991.
[16] V.N. Gubankov, M.P. Lisitskii, I.L. Serpuchenko, F.N. Sklokin and M.V. Fistul, Supercond. Sci. Technol. 5 (1992) 168.